

# Quantum Zeno effect: Quantum shuffling and Markovianity

A. S. Sanz\*, C. Sanz-Sanz, T. González-Lezana, O. Roncero, S. Miret-Artés

*Instituto de Física Fundamental (IFF-CSIC), Serrano 123, 28006 Madrid, Spain*

---

## Abstract

The behavior displayed by a quantum system when it is perturbed by a series of von Neumann measurements along time is analyzed. Because of the similarity between this general process with giving a deck of playing cards a shuffle, here it is referred to as *quantum shuffling*, showing that the quantum Zeno and anti-Zeno effects emerge naturally as two time limits. Within this framework, a connection between the gradual transition from anti-Zeno to Zeno behavior and the appearance of an underlying Markovian dynamics is found. Accordingly, although *a priori* it might result counterintuitive, the quantum Zeno effect corresponds to a dynamical regime where any trace of knowledge on how the unperturbed system should evolve initially is wiped out (very rapid shuffling). This would explain why the system apparently does not evolve or decay for a relatively long time, although it eventually undergoes an exponential decay. By means of a simple working model, conditions characterizing the shuffling dynamics have been determined, which can be of help to understand and to devise quantum control mechanisms in a number of processes from the atomic, molecular and optical physics.

*Key words:* Quantum shuffling, Quantum Zeno effect, Anti-Zeno effect, Measurement theory, von Neumann measurement, Markov chain

---

## 1. Introduction

The legacy of Zeno of Elea becomes very apparent through calculus, the pillar of physics. It is not difficult to find manifestations of his famous paradoxes throughout the subtleties of any of our physical theories [1]. In quantum mechanics, for example, Zeno's paradox of the arrow is of particular interest, for it has given rise to what is now known as quantum Zeno effect (QZE), which constitutes an active field of research [2]. As conjectured by Misra and Sudarshan [3], this effect essentially consists of inhibiting the evolution of an unstable quantum system by a succession of shortly-spaced measurements—a classical analog of this effect is the watched-pot paradox: a watched pot never boils [4]—, although, generally speaking, it could also be a system acted by some environment or even the bare evolution of the system if the latter is not described by a stationary state. The inhibition of the evolution of a quantum system, though, was already noted by von Neumann [5] and others—an excellent account on the historical perspective of the QZE can be found in [2]. From an experimental viewpoint, this effect was formerly detected by Itano *et al.* [6] considering the oscillations of a two-level system, a modification suggested by Cook [7] of the original theoretical proposal. Nonetheless, the first experimental evidences with unstable systems, as originally considered by Misra and Sudarshan, were observed later on by Raizen's group [8, 9]. Indeed, in the second experiment reported by this group in this regard [9], it was also shown the possibility to enhance the system decay by considering measurements more spaced in time. This is the so-called (quantum) anti-Zeno effect (AZE) [10–12].

In the literature, it is common to introduce the QZE and the AZE as antagonist, competing effects. In this work, however, we study their manifestation within a unifying framework, where they constitute the

---

\*Corresponding author

Email address: [asanz@iff.csic.es](mailto:asanz@iff.csic.es) (A. S. Sanz)

two limiting cases of a more general process that we shall refer to as *quantum shuffling*. To understand this concept, consider a series of von Neumann measurements is performed on a quantum system, i.e., measurements such that the outcome has a strong correlation with the measured quantity, thus implying a high degree of certainty on the post-measured system state. This type of measurements provoke the system to collapse into any of the pointer states of the measuring device, breaking the time coherence that characterizes its unitary time-evolution. In other words, the continuity in time between the pre and post-measurement states of the system is irreversibly lost. This loss takes place even when the distance (in time) between the two states is so close that, in modulus, they look pretty much the same, due to the corresponding loss of the phase accumulated with time (which is a signature of the unitary time-evolution and therefore of the possibility to revert the process in time). Thus, consider the system is not stationary (regardless of the nature of the source that leads to such non-stationarity), decaying monotonically in time at a certain rate. A series of measurements on this system will act similarly to giving a deck of ordered cards a shuffle—hence the name of quantum shuffling—, affecting directly its coherence and modifying its natural (unperturbed) decay time-scale. As it is shown here, depending on the relative ratio between the natural time-scale and the shufflingly-modified one, the system decay can be either delayed or enhanced. If the shuffling frequency (i.e., the amount of measurements per time unit) is relatively low with respect to the system natural decay rate, the pre and post-measurement system states will be very different. This turns into a very fast decay due to the important lack of correlation between both states. Within the standard Zeno scenario, this enhancement of the decay corresponds to AZE. On the contrary, if the shuffling is relatively fast, the pre and post-measurement states will be rather similar, for the system did not have time enough to evolve importantly. The decay is then slower, giving rise to QZE. Now, as it is also shown, this inhibition of the system decay is only apparent: the fast shuffling gives rise to an overall exponential decay law at long times that makes the QZE to be sensitive to the total time along which the system is monitored. Thus, in the long term, one just finds out that the system evolution displays features typical of Markovian processes [13], such as exponential decays (with relatively long characteristic times) and time correlation functions with the form of a Markov chain [14]. As a consequence, if the natural system relaxation goes as a decreasing power series with time (e.g., in systems with a regular system dynamics), in the QZE regime it is found that the perturbed system undergoes decays that fall below the natural decay after some time due to the exponential decay induced by the short-spaced measurement process. This unexpected behavior is usually missed and therefore unexplored, since in QZE scenarios it is more common to consider the mathematical limit rather than the physical one.

In order to demonstrate the assertions mentioned above as clearly as possible, here we have considered as a working model the free evolution of a Gaussian wave packet. When it is not perturbed by any measurement, this non-stationary system undergoes a natural decay. That is, this decay is not bound to effects linked to the action of external potentials or surrounding environments, but only to the bare wave-packet spreading as time proceeds. From a time-independent perspective, this spreading is explained by the continuum of frequencies or energies (plane waves) that contribute coherently to the wave packet, which give rise to a non-stationary evolution with time; from a time-dependent view, it is just a diffraction effect associated with the initial *localization* (spatial finiteness) of the wave packet. In either case, this property together with the analyticity and ubiquity of the model (it is a prototypical wave function describing the initial state of atomic, molecular and optical systems) make of the free Gaussian wave packet an ideal candidate to explore the Zeno dynamics. As it is shown, specific conditions for the occurrence of both QZE and AZE are thus obtained in relation to the two mechanisms involved in its dynamics: its translational motion and its intrinsic spreading, which have been shown to rule the dynamics of quantum phenomena, such as interference [15] or tunneling [16]. More specifically, in order to detect QZE and AZE, the overlapping of the wave function at two different times must be non-vanishing. In this regard, therefore, if translation dominates the evolution, the correlation function will decay relatively fast and none of them will be observable. The analytical results here obtained, properly adapted to other contexts, may provide the physical insight necessary to understand more complex processes described by the presence of external interaction potentials or coupled environments [17, 18]. It is also worth stressing that, to some extent, the Zeno regimes found keep a certain closeness with the three-time domain scenario considered by Chiu, Sudarshan and Misra [19].

The work is organized as follows. The dynamics of a free wave packet is introduced in Section 2, in

particular, the (analytical) behavior of its associated time-dependent correlation function. This will provide us with the basic elements to later on establish the conditions leading to QZE or AZE once the shuffling process induced by the succession of measurements will be introduced. In particular, the quantum shuffling effect is analyzed in Section 3 assuming the wave packet is acted by a series of von Neumann measurements. These measurements will be assumed to occur at equally spaced intervals of time and their action on the system will be such that the post-measurement state will always be equal to the initial one. This could be the case, for example, when considering projections (diffractions) through identical slits [20]. Finally, in Section 4 we summarize the main conclusions extracted from this work.

## 2. Dynamics of a free wave packet

### 2.1. Characteristic time scales

Consider the initial state of a quantum system is described in configuration space by the Gaussian wave packet

$$\Psi_0(x) = A_0 e^{-(x-x_0)^2/4\sigma_0^2 + ip_0(x-x_0)/\hbar}, \quad (1)$$

where  $A_0 = (2\pi\sigma_0^2)^{-1/4}$  is the normalization constant,  $x_0$  and  $p_0$  are, respectively, the position and translational (or propagation) momentum of its centroid, and  $\sigma_0$  is its initial spatial spreading. The time-evolution of this wave function in free space ( $V(x) = 0$ ) is given [15] by

$$\Psi_t(x) = A_t e^{-(x-x_t)^2/4\sigma_t^2 + ip_0(x-x_t)/\hbar + iE_0 t/\hbar}. \quad (2)$$

Here,  $A_t = (2\pi\tilde{\sigma}_t^2)^{-1/4}$  is the time-dependent normalization factor;  $x_t = x_0 + v_0 t$  is the time-dependent position of the wave packet centroid, with  $v_0 = p_0/m$  being its speed;  $E_0 = p_0^2/2m$  is the average translational energy, responsible for the time-dependent phase developed by the wave packet as time proceeds; and  $\tilde{\sigma}_t = \sigma_0 [1 + (i\hbar t/2m\sigma_0^2)]$ , with  $\sigma_t = |\tilde{\sigma}_t| = \sigma_0 \sqrt{1 + (\hbar t/2m\sigma_0^2)^2}$  being the time-dependent spreading of the wave packet. This spreading arises [15] from a type of internal or intrinsic kinetic energy, which can be somehow quantified in terms of the so-called spreading momentum,  $p_s = \hbar/2\sigma_0$ , an indicator of how fast the wave packet will spread out. This additional kinetic contribution becomes apparent when analyzing the expectation value of the energy or average energy for the wave packet,

$$\langle \hat{H} \rangle = \frac{p_0^2}{2m} + \frac{p_s^2}{2m}, \quad (3)$$

as well as in the variance,

$$\Delta E \equiv \sqrt{\langle \hat{H}^2 \rangle - \langle \hat{H} \rangle^2} = \sqrt{\frac{2p_s^2}{m}} \sqrt{\frac{p_0^2}{2m} + \frac{p_s^2}{4m}}. \quad (4)$$

(These two quantities are time-independent because of the commutation between Hamiltonian operator,  $\hat{H}$ , and the time-evolution operator,  $\hat{U} = e^{it\hat{H}/\hbar}$ .) From a dynamical point of view, the implications of this term in (3) are better understood through the real phase of (2),

$$S(x, t) = p_0(x - x_t) + \frac{\hbar t}{8m\sigma_0^2\sigma_t^2} (x - x_t)^2 + E_0 t - \frac{\hbar}{2} (\tan)^{-1} \left( \frac{\hbar t}{2m\sigma_0^2} \right). \quad (5)$$

Putting aside the third and fourth terms in these expressions —two space-independent phases related to the propagation and normalization in time, respectively—, we observe that the first term is a classical-like phase associated with the propagation itself of the wave packet, while the second one is a purely quantum-mechanical phase associated with its spreading motion. Correspondingly, each one of these two motions leads to the two energy contributions that we find in (3).

By inspecting the functional dependence of  $\sigma_t$  on time, a characteristic time scale can be defined, namely  $\tau \equiv 2m\sigma_0^2/\hbar$ . This time scale is associated with the relative spreading of the wave packet, allowing us to distinguish three dynamical regimes in its evolution depending on the ratio between  $t$  and  $\tau$  [21]:

- (i) The very-short-time or Ehrenfest-Huygens regime,  $t \lll \tau$ , where the wave packet remains almost spreadless:  $\sigma_t \approx \sigma_0$ .
- (ii) The short-time or Fresnel regime,  $t \ll \tau$ , where the spreading increases nearly quadratically with time:  $\sigma_t \approx \sigma_0 + (\hbar^2/8m^2\sigma_0^3)t^2$ .
- (iii) The long-time or Fraunhofer regime,  $t \gg \tau$ , where the Gaussian wave packet spreads linearly with time:  $\sigma_t \approx (\hbar/2m\sigma_0)t$ .

By means of  $\tau$  we can thus characterize the dynamics of the Gaussian wave packet, although similar time scales could also be found in the case of more general wave packets provided that we have at hand their time-dependent trend —this is in correspondence with the time-domains determined by Chiu, Sudarshan and Misra for unstable systems [19]. Keeping this in mind, consider the probability density associated with (2),

$$|\Psi_t(x)|^2 = \frac{1}{\sqrt{2\pi\sigma_t^2}} e^{-(x-x_t)^2/2\sigma_t^2}. \quad (6)$$

Case (i) is not interesting, because it essentially implies no evolution in time. So, let us focus directly on case (ii), for which (6) reads as

$$|\Psi_t(x)|^2 \approx \frac{1}{\sqrt{2\pi\sigma_0^2}} \left[ 1 - \left( \frac{\hbar^2}{8m^2\sigma_0^4} \right) t^2 \right] e^{-(x-x_t)^2/2\sigma_0^2}, \quad (7)$$

where the time-dependent factor in the argument of the exponential can be neglected without loss of generality (the exponential of such an argument is nearly one). According to (7), the initial falloff of the probability density is parabolic and therefore susceptible to display QZE if a series of measurement is carried out at regular intervals of time [22, 23] provided that these time intervals are, at least,  $\Delta t \lesssim \tau$  (later on, in Section 3, another characteristic time scale, namely the Zeno time, will also be introduced). For longer time scales (case (iii)),

$$|\Psi_t(x)|^2 \approx \sqrt{\frac{2m^2\sigma_0^2}{\pi\hbar^2 t^2}} e^{-(2m^2\sigma_0^2/\hbar^2)(x-x_t)^2/t^2} = \frac{1}{\sqrt{2\pi\sigma_0^2}} \frac{\tau}{t} e^{-(\tau/t)^2(x-x_t)^2/2\sigma_0^2}. \quad (8)$$

Accordingly, for distances such that the ratio  $(x - x_t)/t$  remains constant with time (remember that the spreading is now linear with time), the probability density will decay like  $t^{-1}$ , leading to observe AZE instead of QZE. As it will be shown below in more detail, note that the effect of introducing  $N$  measurements is equivalent (regardless of constants) to having  $t^{-N}$ , which goes rapidly to zero.

## 2.2. Correlation functions and survival probabilities

Now we shall focus on the quantity central to the discussion in this work: quantum correlation function at two different times. Thus, let us consider  $|\Psi_{t_1}\rangle$  generically denotes the state of a quantum system at a time  $t_1$ . The unitary time-evolution of this state from  $t_1$  to  $t_2$  (with  $t_2 > t_1$ ) is accounted for the formal solution of the time-dependent Schrödinger equation

$$|\Psi_{t_2}\rangle = \hat{U}(t_2, t_1)|\Psi_{t_1}\rangle = e^{-i\hat{H}(t_2-t_1)/\hbar}|\Psi_{t_1}\rangle. \quad (9)$$

The quantum time-correlation function is defined as

$$C(t_2, t_1) \equiv \langle \Psi_{t_1} | \Psi_{t_2} \rangle, \quad (10)$$

measuring the correlation existing between the system states at  $t_2$  and  $t_1$ , or, equivalently, after a time  $t = t_2 - t_1$  has elapsed (since  $t_1$ ). This second notion also allows us to rewrite (10) as the correlation function between the wave function at a time  $t = t_2 - t_1$  and the initial wave function ( $t = 0$ ), as it follows from

$$C(t_2, t_1) = \langle \Psi_{t_1} | \Psi_{t_2} \rangle = \langle \Psi_0 | \hat{U}^\dagger(t_1) \hat{U}(t_2) | \Psi_0 \rangle = \langle \Psi_0 | \hat{U}(t_2 - t_1) | \Psi_0 \rangle = \langle \Psi_0 | \Psi_t \rangle = C(t). \quad (11)$$

Another related quantity of interest here is the survival probability,

$$P(t_2, t_1) \equiv |\langle \Psi_{t_1} | \Psi_{t_2} \rangle|^2 = |\langle \Psi_0 | \Psi_t \rangle|^2 = P(t). \quad (12)$$

This quantity indicates how much of the wave function at  $t_1$  still survives at  $t_2$  (in both norm and phase) or, equivalently, how much of the initial wave function (also, in norm and phase) survives at a later time  $t = t_2 - t_1$ . From now on, concerning the Zeno scenario, we are going to work assuming the second approach, although it can be shown that both are equivalent (see Appendix A). Taking this into account together with the general solution (9), the short-time behavior of  $P(t)$  can be readily found,

$$P(t) \approx |\langle \Psi_0 | \left( 1 - \frac{i\hat{H}t}{\hbar} - \frac{\hat{H}^2 t^2}{2\hbar^2} \right) | \Psi_0 \rangle|^2 = 1 - \frac{(\Delta E)^2 t^2}{\hbar^2}, \quad (13)$$

after considering a series expansion up to the second order in  $t$  as well as the normalization of  $\Psi_0$ .

In our case, in particular, the fact that the wave packet spreads along time indicates that the quantum system becomes more delocalized, this making the corresponding correlation function to decay. This can be formally seen by computing the correlation function associated with (2), which reads as

$$C(t) = \sqrt{\frac{2\sigma_0}{\sigma_0 + \tilde{\sigma}_t}} e^{-E_0 t^2 / 2m\sigma_0(\sigma_0 + \tilde{\sigma}_t) - iEt/\hbar} = \left[ 1 + \left( \frac{t}{2\tau} \right)^2 \right]^{-1/4} e^{-E_0 t^2 / 4m\sigma_0^2 [1 + (t/2\tau)^2] + i\delta_t}, \quad (14)$$

with

$$\delta_t = \frac{1}{1 + (t/2\tau)^2} \frac{E_0 t}{\hbar} - \frac{1}{2} (\tan)^{-1} \left( \frac{t}{2\tau} \right). \quad (15)$$

The exponential in (14) only depends on the initial momentum associated with the wave packet centroid, but not on its initial position. This is a key point, for the loss of correlation in a wave function displaying a translation faster than its spreading rate will mainly arise from the lack of spacial overlapping between its values at  $t_1$  and  $t_2$  (or, equivalently, at  $t_0$  and  $t$ ), rather than to the distortion of its shape (and accumulation of phase). However, a relatively slow translational motion will imply that the loss of correlation is mainly due to the wave-packet spreading. In this regard, note how the spreading acts as a sort of intrinsic instability, which is not related at all with the action of an external potential or a coupling to a surrounding environment, but that only comes from the fact that the state describing the system is not stationary (i.e., an energy eigenstate of the Hamiltonian, as it would be the case of a plane wave).

Two scenarios can be thus envisaged to elucidate the mechanisms leading to the natural loss of correlation in a quantum system (at this stage, no measurement is assumed). First, consider  $p_0 = 0$ , i.e., the wave packet only spreads with time, first quadratically and then linearly after the boosting phase [24], as seen in Section 2.1. In this case the correlation function (14) reads as

$$C(t) = [1 + (t/2\tau)^2]^{-1/4} e^{i\varphi_t}, \quad (16)$$

with

$$\varphi_t = -\frac{1}{2} (\tan)^{-1} \left( \frac{t}{2\tau} \right), \quad (17)$$

and the corresponding survival probability (12) as

$$P(t) = \frac{1}{\sqrt{1 + (t/2\tau)^2}}. \quad (18)$$

For short times (case (ii) above), (18) becomes

$$P(t) \approx 1 - \frac{t^2}{8\tau^2}. \quad (19)$$

The functional form displayed by (19) is the typical quadratic-like decay expected for any general quantum state, as it can easily be seen by substituting (4) into the right-hand side of the second equality of (13) with  $p_0 = 0$ . Conversely, at very long times,

$$P(t) \approx \frac{2\tau}{t}, \quad (20)$$

i.e., the survival probability decreases monotonically as  $t^{-1}$ , in correspondence with the result found above for the asymptotic behavior of the probability density. As time evolves, the global phase of the correlation function goes from a linear dependence with time ( $\varphi_t \approx -t/4\tau$ ) to an asymptotic constant value,  $\varphi_\infty = -\pi/4$ . Its value thus remains bound at any time between 0 and  $\varphi_\infty$ .

In the more general case of nonzero translational motion for the wave packet ( $p_0 \neq 0$ ), the survival probability is given by

$$P(t) = \frac{1}{\sqrt{1 + (t/2\tau)^2}} e^{-E_0 t^2 / 2m\sigma_0^2 [1 + (t/2\tau)^2]}. \quad (21)$$

In the short-time limit, this expression reads as

$$P(t) \approx \left(1 - \frac{t^2}{8\tau^2}\right) e^{-E_0 t^2 / 2m\sigma_0^2}. \quad (22)$$

which remarkably stresses the two aforementioned mechanisms competing for the loss of the system correlation: the spreading of the wave packet and its translational motion. This means that if the translational motion is faster than the spreading rate, the wave functions at  $t_0$  and  $t$  will not overlap, and  $P(t)$  will vanish very fast. On the contrary, if the translational motion is relatively slow, the overlapping will be relevant and the decay of  $P(t)$  will go quadratically with time. In order to express the relationship between spreading and translation more explicitly, (22) can be expressed in terms of  $p_0$  and  $p_s$ , i.e.,

$$P(t) \approx \left(1 - \frac{t^2}{8\tau^2}\right) e^{-2(p_0/p_s)^2 (t^2/8\tau^2)}. \quad (23)$$

Thus, if the translational and spreading motions are such that

$$\frac{p_0}{p_s} \ll \frac{2\tau}{t} \quad (24)$$

(actually, it is enough that  $p_0/p_s \lesssim 1/\sqrt{2}$ , since  $t^2/8\tau^2$  is already relatively small), then

$$P(t) \approx 1 - \left[1 + 2\left(\frac{p_0}{p_s}\right)^2\right] \frac{t^2}{8\tau^2}, \quad (25)$$

which again decays quadratically with time. Otherwise, the decrease of  $P(t)$  will be too fast to observe either QZE or AZE (see below). Regarding the long-time regime, we find

$$P(t) \approx \frac{2\tau}{t} e^{-2E\tau^2/m\sigma_0^2} = \frac{2\tau}{t} e^{-(p_0/p_s)^2}, \quad (26)$$

which displays the same decay law ( $t^{-1}$ ) as in the case  $p_0 = 0$ , since the argument of the exponential function becomes constant. Regarding the phase  $\delta_t$ , it should be mentioned that at short times it depends linearly with time, increasing or decreasing depending on which mechanism (translation or spreading) is stronger. However, at longer times it approaches asymptotically (also like  $t^{-1}$ ) the value  $\varphi_\infty$  regardless of which mechanism is the dominant one.

### 3. Quantum Zeno effect and projection operations

In the standard QZE scenario, a series of von Neumann measurements are performed on the system at regular intervals of time  $\Delta t$ . Between two any consecutive measurements the system follows a unitary time-evolution according to (9), while each time a measurement takes place (at times  $t = n\Delta t$ , with  $n = 1, 2, \dots$ ) the unitarity of the process breaks down and the system quantum state “collapses” into one of the pointer states of the measuring device. With this scheme in mind, consider the pointer states are equal to the system initial state—in the case we are analyzing here, this type of measurements could consist, for example, of a series of diffractions produced by slits with similar transmission properties to the one that generated the initial wave function [20]. Thus, after the first measurement the system state will be

$$|\Psi_{t=\Delta t}\rangle = |\Psi_0\rangle\langle\Psi_0|\Psi_{\Delta t}\rangle, \quad (27)$$

which coincides with the initial state, although its amplitude is decreased by a factor  $\langle\Psi_0|\Psi_{\Delta t}\rangle$ . Each new measurement will therefore add a multiplying factor  $|\langle\Psi_0|\Psi_{\Delta t}\rangle|^2$  in the survival probability, which implies that it will read as

$$P_n(t) = \left[\mathcal{P}_{\Delta t}^{(0)}\right]^n |\langle\Psi_0|\Psi_{t-n\Delta t}\rangle|^2 \quad (28)$$

after  $n$  measurements, where  $\mathcal{P}_{\Delta t}^{(0)} \equiv |\langle\Psi_0|\Psi_{\Delta t}\rangle|^2$ . For  $\Delta t$  sufficiently small,  $\mathcal{P}_{\Delta t}^{(0)}$  acquires the form of (13),

$$\mathcal{P}_{\Delta t}^{(0)} \approx 1 - \frac{(\Delta E)^2(\Delta t)^2}{\hbar^2}, \quad (29)$$

from which another characteristic time arises, namely the *Zeno time* [2], defined as

$$\tau_Z \equiv \frac{\hbar}{\Delta E}. \quad (30)$$

In Section 2.1, different stages in the natural evolution of the quantum system were distinguished given the ratio between  $t$  and the time scale  $\tau$ . The new time scale provided by  $\tau_Z$  also allows us to distinguish between two types of dynamical behavior. For measurements performed at intervals such that  $\Delta t \ll \tau_Z$ , (29) holds and the decay of the perturbed correlation function will be relatively slow with respect to the total time the system is monitored. Traditionally, this defines the Zeno regime, where the decay of the correlation function is said to be inhibited due to the measurements performed on the system. On the contrary, as  $\Delta t$  becomes closer to  $\tau_Z$ , (29) does not hold anymore and the decay of the correlation function becomes faster than the unperturbed one for finite  $t$ .

In the case of a free Gaussian wave packet with  $p_0 = 0$  (the system dynamics is only ruled by the wave packet spreading), substituting (4) into (30) the Zeno time can be expressed as

$$\tau_Z = 2\sqrt{2}\tau, \quad (31)$$

which is nearly three times larger than  $\tau$ . According to the standard scenario, provided that  $\Delta t$  is smaller than  $\tau_Z$ , one should observe QZE. However, the characteristic time  $\tau$  also plays a key role: as shown below, QZE is observable provided that measurements are performed at time intervals much shorter than the time scales ruling the wave-packet linear spreading regime. Otherwise, only AZE will be observed. If now we consider the more general case, where the free wave packet has an initial momentum ( $p_0 \neq 0$ ), a more stringent condition is obtained. According to (25)—or, equivalently, substituting (4) into definition (30)—, we find

$$\tau_Z = \frac{2\sqrt{2}\tau}{\sqrt{1 + 2(p_0/p_s)^2}}, \quad (32)$$

which implies that, in order to observe QZE, the time intervals  $\Delta t$  between two consecutive measurements have to be even shorter (apart from the fact that the condition  $p_0/p_s \lesssim 1/\sqrt{2}$  should also be satisfied). This condition ensures that the wave function at  $t$  still has an important overlap with its value at  $t_0$ .

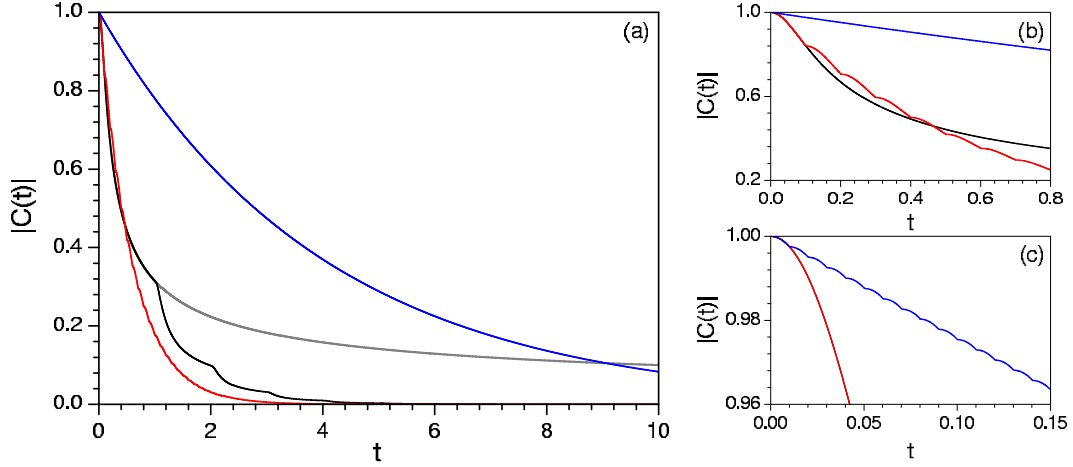


Figure 1: (a) Modulus of the time correlation function,  $|C(t)|$ , for the unperturbed system (gray line) and three different cases with measurements performed at:  $\Delta t_1 = 10^4 \delta t = 1$  (black),  $\Delta t_2 = 10^3 \delta t = 0.1$  (red), and  $\Delta t_3 = 10^2 \delta t = 0.01$  (blue), with  $\delta t = 10^{-4}$  being the time-step considered in the simulation. (b) and (c) are enlargements of part (a) for times of the order of  $\tau_Z$  and  $\tau$ , respectively. In the calculations,  $m = 0.1$ ,  $\sigma_0 = 0.5$  and  $p_0 = 0$ , which render  $\tau = 0.05$  and  $\tau_Z = 0.14$  (see text for details).

With the tools developed so far, let us now have a closer look at the QZE and AZE dynamics. Typically, these effects are assumed to be quite the opposite. However, we show they constitute the two limits of the aforementioned quantum shuffling process. For simplicity and without loss of generality, instead of considering the survival probability, in Fig. 1(a) we have plotted the modulus of the time correlation function,  $|C(t)|$ , against time to monitor the natural (unperturbed) evolution of the wave packet (gray curve) and three cases where measurements have been performed at different time intervals  $\Delta t$ . These intervals have been chosen proportional to the time-step  $\delta t$  ( $= 10^{-4}$  time units) used in the numerical simulation:  $\Delta t_1 = 10^4 \delta t = 1$  (black),  $\Delta t_2 = 10^3 \delta t = 0.1$  (red), and  $\Delta t_3 = 10^2 \delta t = 0.01$  (blue). Regarding other parameters, we have used  $m = 0.1$ ,  $\sigma_0 = 0.5$  and  $p_0 = 0$ , which make  $\tau = 0.05$  and  $\tau_Z \approx 0.14$ . The three color curves displayed in Fig. 1(a), which show the action of a set of measurements on the quantum system, behave in a similar fashion: they are piecewise functions, each piece being identical to the corresponding one between  $t = 0$  and  $t = \Delta t$ , i.e., to  $C_{\Delta t}^{(0)} \equiv \sqrt{\mathcal{P}_{\Delta t}^{(0)}}$ . These curves allow us to illustrate the quantum shuffling process in three time regimes which depend on the relationship between  $\tau$ ,  $\tau_Z$  and  $\Delta t$ :

- (a) For  $\tau < \tau_Z \leq \Delta t$ , the correlation function (see the black curve in Fig. 1(a)) is clearly out of the quadratic-like time domain,  $C_{\Delta t}^{(0)}$  is convex and therefore the perturbed correlation function *always* goes to zero much faster than the natural decay law (gray curve). This is what we call *pure AZE*, for the correlation function is always decaying below the unperturbed function.
- (b) For  $\tau \leq \Delta t \leq \tau_Z$ , according to the literature one should observe QZE. However, this is not exactly the case. Between  $\tau$  and  $\tau_Z$ , the correlation function (18) displays an inflection point at  $\tau_{\text{infx}} = \sqrt{2}\tau \approx 0.071$ , changing from convex to concave. Thus, for  $\Delta t$  between  $\tau_{\text{infx}}$  and  $\tau_Z$ , pure AZE is still found due to the convexity of the time correlation function. Now, if  $\tau \leq \Delta t \leq \tau_{\text{infx}}$ , the initial falloff of the perturbed correlation function is slower,  $C_{\Delta t}^{(0)}$  becomes concave and the overall decay gets slower than that associated with the unperturbed correlation function (see red curve in Fig. 1(a)). This lasts out for some time, after which the perturbed correlation function falls below the unperturbed one (see red curve in Fig. 1(b)). It is worth stressing here how the decay is indeed faster than in the case of pure AZE, with the quantum shuffling making the perturbed correlation function to acquire a seemingly exponential-like shape.
- (c) For  $\Delta t < \tau$ , the wave packet is well inside the region where the wave function decay is quadratic-like (and concave) and therefore the quantum shuffling produces decays much slower than those observed in the unperturbed correlation function as  $\Delta t$  decreases (see blue curve in Fig. 1(c)). This is commonly



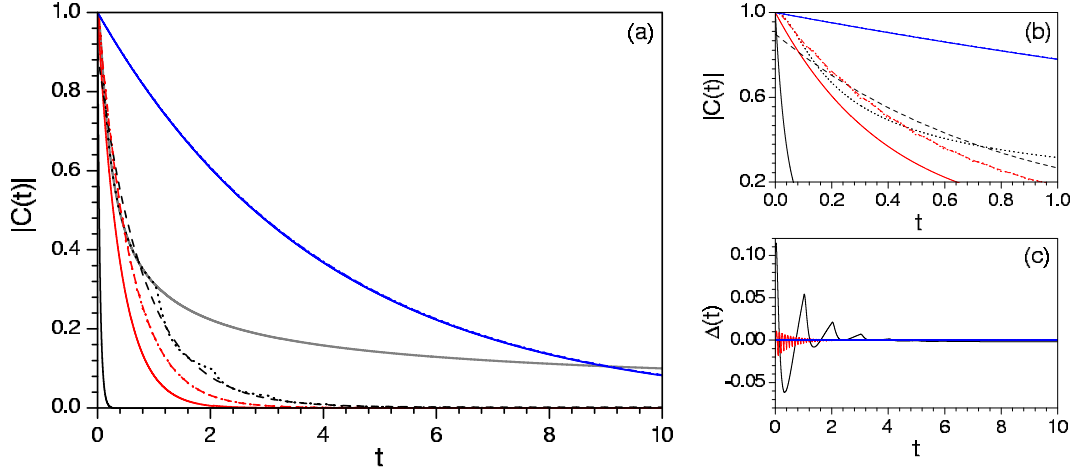


Figure 2: (a) Same as Fig. 1(a), but showing the envelope (36) superimposed to the corresponding perturbed decay functions:  $\Delta t_1 = 1$  (black),  $\Delta t_2 = 0.1$  (red) and  $\Delta t_3 = 0.01$  (blue). In the figure, the different types of line denote the modulus of the time correlation function,  $|C(t)|$ , obtained from: the simulation (dotted), the theoretical estimation (36) (solid), and the fitting to a pure exponential function (dashed); to compare with, the unperturbed correlation function is also displayed with gray line in panel (a). The decay rates arising from the theoretical estimation are  $\gamma'_{1,\text{est}} = 25$  (black),  $\gamma'_{2,\text{est}} = 2.5$  (red) and  $\gamma'_{3,\text{est}} = 0.25$  (blue), while those obtained from the fitting are  $\gamma'_{1,\text{fit}} = 1.224$  (black),  $\gamma'_{2,\text{fit}} = 1.734$  (red) and  $\gamma'_{3,\text{fit}} = 0.249$  (blue). (b) Enlargement of part (a) in the time interval between  $t = 0$  and  $t = 1$ . (c) Plot of the difference  $\Delta(t)$  between the estimated envelope,  $C_{\Delta t}(t)$ , and the fitted envelope, in part (a).

known as QZE. Now, this inhibition of the decay is only apparent; if one considers longer times (see blue curve in Fig. 1(a)), the correlation function is essentially a decreasing exponential, which eventually leads the (perturbed) system to decay to zero earlier than its unperturbed counterpart. As it will be shown below, these exponential decays can be justified in terms of a sort of Markovianity induced by the shuffling process on the system evolution.

In order to better understand the subtleties behind the quantum shuffling dynamics (and therefore the QZE and the AZE), let us focus only on the overall prefactor that appears in (28), which in the short-time regime can be written as

$$\mathcal{P}_{\Delta t}^{(n)} \equiv [\mathcal{P}_{\Delta t}^{(0)}]^n \approx \left[1 - \frac{(\Delta t)^2}{\tau_Z^2}\right]^n. \quad (33)$$

This is a discrete function of  $n$ , the number of measurements performed up to  $t_n \equiv n\Delta t$ , the time at which the  $n$ -th measurement is carried out. In the limit  $n \rightarrow \infty$ , (33) becomes

$$\mathcal{P}_{\Delta t}^{(\infty)}(t_n) \approx e^{-\gamma_{\Delta t} t_n}, \quad (34)$$

with the decay rate being

$$\gamma_{\Delta t} \equiv \frac{\Delta t}{\tau_Z^2}, \quad (35)$$

as also noted in [2]. This rate defines another characteristic time,  $\tau_{\Delta t} \equiv \gamma_{\Delta t}^{-1}$ , associated with the falloff of the continuous form of (34),

$$\mathcal{P}_{\Delta t}(t) = e^{-\gamma_{\Delta t} t} \quad (36)$$

(note that this function passes through all the points  $t_n$  upon which (34) is evaluated). In Fig. 2 we show a comparative analysis between the correlation functions  $|C(t)|$  displayed in Fig. 1 and their respective envelopes, given by  $\mathcal{C}_{\Delta t}(t) \equiv \sqrt{\mathcal{P}_{\Delta t}(t)}$ ; the former are denoted with dotted line and the latter with solid line of the same color (again, the gray solid line represents the unperturbed correlation function). The

values for the estimated decay rates, given by  $\gamma'_{\Delta t} = \gamma_{\Delta t}/2$  for the curves represented, are:  $\gamma'_1 = 25$  (black),  $\gamma'_2 = 2.5$  (red) and  $\gamma'_3 = 0.25$  (blue). As it can be seen, the agreement between the correlation function and its envelope  $\mathcal{C}_{\Delta t}(t)$  becomes better as  $\Delta t$  decreases (see Figs. 2(a) and (b)), which is in virtue of the approximation considered in (33) —as  $\Delta t$  increases the behavior of the envelope (36) will diverge more remarkably with respect to the trend displayed by  $P_n(t)$ , whereas both will converge as  $\Delta t$  becomes smaller. Thus, while for long intervals  $\Delta t$  between consecutive measurements the envelope deviates importantly from the associated correlation function (see black dotted and solid lines), as  $\Delta t$  becomes smaller the difference between both curves reduces importantly and the relaxation takes longer times (of the order of  $\tau_{\Delta t}$ ). Nevertheless, for larger values of  $\Delta t$  one can still perform a fitting of the correlation function to a decaying exponential function,  $\mathcal{C}_{\Delta t, \text{fit}}^{(\infty)}(t) = e^{-\gamma'_{\text{fit}} t}$ , which renders a qualitatively good overall agreement, as can be seen from the corresponding dashed lines in Fig. 2(a). Note that the decay rates obtained from this fitting are closer to the falloff observed for the corresponding correlations functions ( $\gamma'_{1, \text{fit}} = 1.224$ ,  $\gamma'_{2, \text{fit}} = 1.734$ , and  $\gamma'_{3, \text{fit}} = 0.249$ ), converging to the estimated value  $\gamma'$  as  $\Delta t$  decreases ( $\gamma'_{3, \text{fit}} \approx \gamma'_3$ ).

From the previous discussion, the idea of a series of sequential measurement acting as a shuffling process, wiping out any memory of the system past history, arises in a natural way. Hence, as  $\Delta t$  becomes smaller,  $|C(t)|$  becomes closer to its envelope  $\mathcal{C}_{\Delta t}(t)$  and therefore to an exponential decay law. Conversely, for larger values of  $\Delta t$ , the system keeps memory of its past evolution for relatively longer periods of time (between two consecutive measures), this leading to larger discrepancies between the correlation function and (36). Taking into account this point of view and getting back to (28), one can notice a remarkable resemblance between this expression and a Markov chain of independent processes [14] (which is also inferred from (34)): the state after one measurement only depends on the state before it, but not on the previous history or sequence until this state is reached. That is, between any two consecutive measurements we have a precise knowledge of the probability to find the system in a certain time-dependent state, while, after a measurement, we loose any memory on that. Thus, as  $\Delta t$  becomes smaller, the process becomes fully Markovian, with the time correlation function approaching the typical exponential-like decreasing behavior characteristic of this type of processes. On the contrary, as  $\Delta t$  increases, the memory on the past history is kept for longer times, this turning the system evolution into non-Markovian, which loses gradually the smooth exponential-like decay behavior. Only when a measurement is carried out such memory is suddenly removed, which is the cause of the faster (sudden) decays observed in black curve of Fig. 1(a).

The transition from the non-Markovian to the Markovian regime can be somehow quantified by monitoring along time the distance between the estimated envelope,  $\mathcal{C}_{\Delta t}(t)$ , and the fitted envelope,  $\mathcal{C}_{\Delta t, \text{fit}}(t)$ ,

$$\Delta(t) \equiv \mathcal{C}_{\Delta t}(t) - \mathcal{C}_{\Delta t, \text{fit}}(t), \quad (37)$$

which is plotted in Fig. 2(c) for the three cases of  $\Delta t$  considered. Thus, as  $\Delta t$  becomes smaller, we approach an exponential decay law and  $\Delta(t)$  goes to zero for any time (see blue curve in the figure), this being the signature of Markovianity. On the contrary, if the time evolution is not Markovian, as time increases and the system keeps memory for longer times, the value of  $\Delta(t)$  displays important deviations from zero (see black and red curves in the figure). These deviations mainly concentrate on the short and medium term dynamics, where values are relatively large to be remarkable. Nonetheless, analogously, one could also display the relative ratio between the two correlation functions, which would indicate or not the trend toward Markovianity in the long-time (asymptotic) regime.

#### 4. Conclusions

By assuming that the QZE inhibits the evolution of an unstable quantum system, one might also be tempted to think that its coherence is also preserved, while the AZE would lead to the opposite effect in its way through faster system decays. In order to better understand these effects, here we have focused directly on the bare system, i.e., no external potentials or surrounding environments acting on the quantum system have been assumed. This has allowed us to elucidate the conditions under which such effects take place in relation to the intrinsic time-scales characterizing the isolated system, which have been shown to play an important role. Furthermore, by means of this analysis, we have also shown that both QZE and AZE are

indeed two instances of a more general effect, namely a *quantum shuffling process*, which eventually leads the system to display a Markovian-like evolution and its correlation function to follow an exponential decay law as the interval between measurements decreases. Within this scenario, the QZE dynamics can be regarded as a regime where any trace of knowledge on the initial system state is lost due to a rapid shuffling, while in the long-time regime the correlation function would fall to zero faster than the unperturbed one. The apparent contradiction with the traditional no-evolution scenario can be explained very easily: Since one often cares only about the short-time dynamics, the long-time dynamics is usually completely neglected. In other words, the time during which the system dynamics is usually studied is relatively small compared to the Markovian time-scale induced by the continuous measurement process and, therefore, one assumes nearly stationary dynamics.

## Acknowledgements

The support from the Ministerio de Ciencia e Innovación (Spain) through Projects FIS2010-18132, FIS2010-22082, CSD2009-00038; from Comunidad Autónoma de Madrid through Grant No. S-2009/MAT/1467; and from the COST Action MP1006 (*Fundamental Problems in Quantum Physics*) is acknowledged. A. S. Sanz also thanks the Ministerio de Ciencia e Innovación for a “Ramón y Cajal” Research Fellowship.

## A. Alternative Zeno scenario

In the Zeno scenario considered above, establishing a direct analogy with Zeno’s arrow, the wave packet plays the role of a quantum arrow, but with the particularity that this arrow slows down until its evolution is frozen by means of a series of measurements. This is the scenario traditionally considered [2]. However, a more direct analogy with Zeno’s arrow paradox can be established if it is assumed that the wave packet is always in motion and the measurements are just like photographs indicating the particular instant from which the correlation has to be computed [18]. Because of the actions on the wave packet in relation to what a measurement is considered in each, we can call these two situations as:

- (a) The *stopping-arrow scenario*, where the wave packet is “collapsed” or “stopped” after each measurement.
- (b) The *steady-arrow scenario*, where the wave packet time-evolution never stops, but the computation of the correlation function is reset after each (photograph-like) measurement —like in a stop-motion or stop-action movie.

It can be shown that both scenarios are equivalent with the exception of a lost time-dependent phase in the latter. In order to prove this statement, let us start by considering the wave function is now left to freely evolve in time. Following the idea behind this scenario, the survival probability is monitored in time by computing the overlapping of the wave function at a time  $t$  with its value at successive times  $t_0, t_1, t_2$ , with  $t_n = n\Delta t$ , i.e.,

$$\langle \Psi_{t_{n-1}} | \Psi_t \rangle, \quad (38)$$

where  $t_{n-1} \leq t < t_n$ . Note here the direct analogy with Zeno’s arrow, where at each instant we are observing the arrow steady at a different space position, but without freezing its motion. Taking this into account, for  $0 \leq t < t_1$ , we have

$$P(t) = |\langle \Psi_0 | \Psi_t \rangle|^2. \quad (39)$$

Now, if  $t_1 \leq t < t_2$ ,

$$P(t) = \alpha_1 |\langle \Psi_{t_1} | \Psi_t \rangle|^2, \quad (40)$$

while the wave function for the same interval will be

$$|\Psi_t\rangle = \sqrt{\alpha_1} |\Psi_t\rangle, \quad (41)$$

i.e., the evolved wave function, but with a prefactor which ensures the matching of the different of  $P(t)$  before and after  $t = t_1$ . Following the same argumentation, after the  $n - 1$  measurement,

$$P(t) = \left( \prod_{k=1}^{n-1} \alpha_k \right) |\langle \Psi_{t_{n-1}} | \Psi_t \rangle|^2, \quad (42)$$

with  $t_{n-1} \leq t \leq t_n$ .

As it can be seen, by means of this procedure the wave function is never altered (which always keeps evolving according to the Schrödinger equation), but only its relative amplitude. So, the key issue here is the attenuation factor  $\alpha$ , which can be evaluated as follows. For  $t_{n-1} \leq t < t_n$ , we note that

$$\langle \Psi_{t_{n-1}} | \Psi_t \rangle = \langle \Psi_0 | e^{i\hat{H}(n-1)\Delta t/\hbar} e^{-i\hat{H}t/\hbar} | \Psi_0 \rangle = \langle \Psi_0 | e^{i\hat{H}[t-(n-1)\Delta t]/\hbar} | \Psi_0 \rangle. \quad (43)$$

Therefore, the attenuation factor for the interval  $t_{n-1} \leq t \leq t_n$  should come from the overlapping of the wave function at the times when the two previous measurements were performed, i.e.,

$$\alpha_{n-1} = |\langle \Psi_{t_{n-2}} | \Psi_{t_{n-1}} \rangle|^2 = |\langle \Psi_0 | e^{i\hat{H}\Delta t/\hbar} | \Psi_0 \rangle|^2. \quad (44)$$

This expression can be Taylor expanded to second order in  $\Delta t$  (assuming  $\Delta t$  is small enough) taking into account that

$$\langle \Psi_0 | \Psi_{\Delta t} \rangle \approx 1 - \frac{i\tau_Z}{\hbar} \langle \Psi_0 | \hat{H} | \Psi_0 \rangle + \frac{\tau_Z^2}{2\hbar^2} \langle \Psi_0 | \hat{H}^2 | \Psi_0 \rangle, \quad (45)$$

where we have assumed the wave function is initially normalized. This renders

$$\alpha_n = |\langle \Psi_0 | \Psi_{t_1} \rangle|^2 \approx 1 - \frac{(\Delta t)^2}{\hbar^2} \left( \langle \Psi_0 | \hat{H}^2 | \Psi_0 \rangle - \langle \Psi_0 | \hat{H} | \Psi_0 \rangle^2 \right) = 1 - \frac{(\Delta t)^2}{\hbar^2} (\Delta \hat{H})^2, \quad (46)$$

which is valid for any  $n$ , since it does not depend explicitly on the particular time at which the measurement is made. Therefore, (42) can be expressed as

$$P(t) = \alpha_1^{n-1} |\langle \Psi_{t_{n-1}} | \Psi_t \rangle|^2, \quad (47)$$

which is formally equivalent to (28) after performing  $n$  measurements, although it describes a completely different physics [18].

## References

- [1] J. Mazur, *Zeno's Paradox: Unraveling the Ancient Mystery behind the Science of Space and Time*, Plume, New York, 2007.
- [2] P. Facchi, S. Pascazio, *J. Phys. A: Math. Theor.* 41 (2008) 493001.
- [3] B. Misra, E. C. G. Sudarshan, *J. Math. Phys.* 18 (1977) 756.
- [4] A. Peres, *Am. J. Phys.* 48 (1980) 931.
- [5] J. von Neumann, *Die Mathematische Grundlagen der Quantenmechanik*, Springer Verlag, Berlin, 1932.
- [6] W. M. Itano, D. J. Heinzen, J. J. Bollinger, D. J. Wineland, *Phys. Rev. A* 41 (1990) 2295.
- [7] R. J. Cook, *Phys. Scr.* T21 (1988) 49.
- [8] S. R. Wilkinson, C. F. Bharucha, M. C. Fischer, K. W. Madison, P. R. Morrow, Q. Niu, B. Sundaram, M. G. Raizen, *Nature* 387 (1997) 575.
- [9] M. C. Fischer, B. Gutiérrez-Medina, M. G. Raizen, *Phys. Rev. Lett.* 87 (2001) 040402.
- [10] B. Kaulakys, V. Gontis, *Phys. Rev. A* 56 (1997) 1131.
- [11] A. Luis, L. Sánchez-Soto, *Phys. Rev. A* 57 (1998) 781.
- [12] A. G. Kofman, G. Kurizki, *Nature* 405 (2000) 546.
- [13] H.-P. Breuer, F. Petruccione, *The Theory of Open Quantum Systems*, Oxford University Press, Oxford, 2002.
- [14] P. E. Kloeden, E. Platen, *Numerical Solution of Stochastic Differential Equations*, Springer, Berlin, 1992.
- [15] A. S. Sanz, S. Miret-Artés, *J. Phys. A: Math. Theor.* 41 (2008) 435303.
- [16] A. S. Sanz, S. Miret-Artés, *J. Phys. A: Math. Theor.* 44 (2011) 485301.
- [17] C. Sanz-Sanz, A. S. Sanz, T. González-Lezana, O. Roncero, S. Miret-Artés, (submitted for publication, 2011); eprint arXiv:1106.4143.
- [18] C. Sanz-Sanz, A. S. Sanz, T. González-Lezana, O. Roncero, S. Miret-Artés, (submitted for publication, 2011); eprint arXiv:1111.1520.
- [19] C. B. Chiu, E. C. G. Sudarshan, B. Misra, *Phys. Rev. D* 16 (1977) 520.
- [20] M. A. Porras, A. Luis, I. Gonzalo, A. S. Sanz, *Phys. Rev. A* 84 (2011) 052109.
- [21] A. S. Sanz, S. Miret-Artés, *Am. J. Phys.* (at press, 2011); eprint arXiv:1104.1296.
- [22] E. Donkor, A. R. Pirich, H. E. Brandt (Eds.), *Quantum Zeno and anti-Zeno effects: An exact model*, in: Society of Photo-Optical Instrumentation Engineers (SPIE) Conference Series, vol. 5436, SPIE, Bellingham, WA, 2004; eprint arXiv:quant-ph/0501098.
- [23] H. C. Peñate-Rodríguez, R. Martínez-Casado, G. Rojas-Lorenzo, A. S. Sanz, S. Miret-Artés, *J. Phys.: Condens. Matter* (at press, 2011); eprint arXiv:1104.1294.
- [24] A. S. Sanz, S. Miret-Artés, *Chem. Phys. Lett.* 445 (2007) 350.